JOURNAL OF MATERIALS SCIENCE **38** (2003) 2489–2498

Time-dependent aspects of the mechanical properties of plant and vegetative tissues

H. X. ZHU*
Polymer and Colloids Group, Cavendish Laboratory, Cambridge University, Madingley Road, Cambridge CB3 0HE, UK
E-mail: hz207@cam.ac.uk

J. R. MELROSE
Unilever Research, Colworth House, Sharnbrook, Beds MK44 1LQ, UK

Based on a single regular cell structural model, the effects of loading rate on the compressive behaviour of plant and vegetative tissues have been qualitatively investigated. The cell walls were treated as a polymeric composite material with microfibrils embedded in the highly structured cell wall matrix. The rubber elasticity, the turgor permeability and the loading rate were taken into account to qualitatively predict the tissue stiffness, cell wall stress, turgor pressure, cell debonding force, and the percentage of weight loss of the cell fluid. The predicted results are consistant with the related experimental phenomena.

1. Introduction

Fruit and vegetables are food products. It has long been recognised that freezing and cooking can dramatically change the structural and mechanical properties of plant and vegetable tissues [1–3], and those properties are directly related to oral sensory perception. In raw (unprocessed) fruit and vegetables, the fluid is retained by the cell membrane inside the cell walls. Cell membrane is the lipidbilayer containing the cell. Cell wall is cellulosic fibre composite. When plant and vegetables are processed by freezing or cooking, the cell membrane can be destroyed in different degrees, and the fluid can express through the cell walls. Hence, the mechanical properties of the processed plant and vegetable tissues are loading-rate dependent.

Relatively low loading rates have been studied in raw materials [1, 4–9], while in-mouth deformation rates are usually very high [10–12]. To link the mechanical and sensory properties of a plant or vegetable tissue, a wide range of strain rate should be considered. In processed plant and vegetables, if the loading rate is very low, the fluid in the tissue is relatively free to flow through the cell walls, hence the internal pressure can not be built up in the tissue. If the loading rate is high enough, the fluid in the tissue could be trapped in the cells and the tissue behaves in a similar way to the raw (unprocessed) tissue. Theoretical and experimental results indicate that both the tissue stiffness and the cell wall stress increase with increasing cell turgidity [13–16]. Hence, increasing the loading rate or the turgor pressure decreases the compressive stress at failure of the tissues, such as potato and apple [17, 18].

Although some experimental work has been carried out to investigate the effects of loading rate on the mechanical properties of plant and vegetable tissues, very little theoretical analysis has been done to predict the mechanical behaviour of plant and vegetable tissue. Using a two dimensional hexagonal cell model and assuming that the cell wall material is linear elastic, Pitt and Chen [19] have qualitatively analysed the effects of loading rate on the mechanical response of vegetative tissues. However, the cell walls of plant or vegetables are polymeric composite materials with microfibrils embedded in the highly structured cell wall matrix. The aim of this work is to qualitatively relate fluid diffusion, loading rate, and the cell wall elasticity to the mechanical behaviour of the whole tissue of plant or vegetables. The analysis is based on a three dimensional hexagonal cell structural model. The cell walls are treated as a rubber-like (polymeric) material, and the case of cell walls with microfibrils stiffening has been taken into account. The emphasis is focused on the mechnaical properties, hence the extremely complex situation in the living cells has been greatly simplified in this analysis. However, the analytical results should give qualitative insight into the response of the actual tissue.

2. Model development

The model and the analysis developed in this paper are the direct extension of our previous work [16]. As before, we use an array of identical, regular three dimensional hexagonal cells to present the plant or

* *Present Address:* Micromechanics Centre, Department of Engineering, University of Cambridge, Cambridge CB2 1PZ, UK.

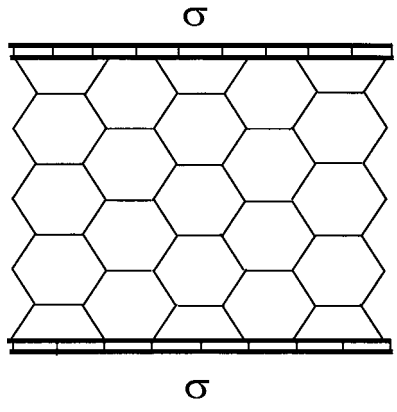

(a)

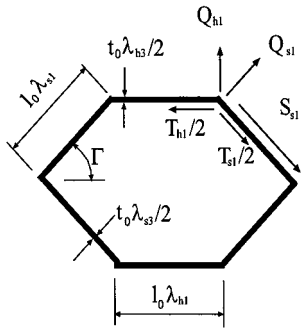

(b)

Figure 1 (a) Two-dimensional projection of a cellular tissue of plant or vegetable as thin-walled, fluid-filled shells; (b) Cell wall tensions T_{h1} and T_{s1}, intercellular debonding tensions Q_{h1} and Q_{s1}, intercellular shear stress S_{s1}, the characteristic angle Γ and the cross-sectional dimensions of a deformed cell.

vegetable tissue (see Fig. 1a). The cells are thin-walled (less than 10 percent by volume, [20]) and fluid-filled vessels with a positive internal turgor pressure. Each cell wall is shared by the two neighbouring cells (actually each cell has its own primary cell wall, however, the "cell wall" we adopt here in the mechanics models consists of the two primary walls of the neighbouring cells, which are glued by a much thinner layer of middle lamella). The cell walls are assumed to be a composite material, consisting of matrix and microfibrils. The polymer-based cell wall matrix is comparatively amorphous in structure [21–23], hence, it is assumed to be mechanically isotropic. The microfibrils embedded in the matrix consist of highly structured, crystalline cellulose-based polymer strands of low extensibility. These strands withstand stress with a minimum of stretching [22] and by re-orientation. The microfibrils have different elastic properties in different directions due to different structural arrangements of their constituent polymer molecules. The cell walls are supposed to be uniform in thickness for each face and treated as a mechanically homogenous polymeric composite material with microfibrils embedded in the matrix. Owing to the fact that the cell walls are made of polymers, they are assumed to be conserved in volume (i.e. $\lambda_1\lambda_2\lambda_3 = 1$, λ_1, λ_2 and λ_3 are the three principle extension ratios of the cell wall materials), and therefore polymer mechanics can be applied. For a homogeneous, isotropic and incompressible elastic material, as long as the strain energy function W is known, the three principal *Cauchy* stresses can be expressed by [24]

$$\tau_i = \lambda_i \frac{\partial W}{\partial \lambda_i} + p \tag{1}$$

where, p is an arbitrary hydrostatic stress due to the fact that an arbitrary hydrostatic stress does not contribute to the deformation energy.

Not all non-linear elastic materials have a strain-energy function. Those that do are called hyperelastic materials. The derivation of the strain energy function is based on either experimental measurement or structural molecular theory. For isotropic materials, the strain energy W can be expressed as functions of the strain invariants I_1 and I_2 (and $I_3 = 1$), such as the Rivlin series [25]. However, the mechanical properties of the cell walls of plant or vegetable tissues are different in different directions due to the microfibrillar stiffening. This is incorporated into the analysis by defining *directional microfibrillar stiffening factors* k_1 *and* k_2 respectively for the circumferential and the axial directions. In the remaining third direction (i.e. the cell wall thickness direction) there are no microfibrillar restrictions to prevent wall thinning during expansion, hence $k_3 = 1.0$. The stiffening of the microfibrils can be incorporated into the pseudo-strain-energy function of the cell wall materials, and given by

$$\begin{aligned} W = C_1\big(\big(\big(k_1\big(\lambda_1^2 - \ln\lambda_1^2\big) + k_2\big(\lambda_2^2 - \ln\lambda_2^2\big) \\ + k_3\big(\lambda_3^2 - \ln\lambda_3^2\big) - (k_1 + k_2 + k_3)\big) \\ + \alpha\big(k_1\big(1/\lambda_1^2 + \ln\lambda_1^2\big) + k_2\big(1/\lambda_2^2 + \ln\lambda_2^2\big) \\ + k_3\big(1/\lambda_3^2 + \ln\lambda_3^2\big) - (k_1 + k_2 + k_3)\big)\big) \end{aligned} \tag{2}$$

where, C_1 and α are the material constants of the cell wall matrix, and λ_1, λ_2 and λ_3 are the three principle extension ratios of the cell wall material. As mentioned in our previous work [16], this pseudo-strain-energy function (Equation 2) is logically possible because $W = 0$ when $\lambda_1 = \lambda_2 = \lambda_3 = 1$ (this is for the undeformed state), and W increases with increasing deformation when $\lambda_1 \geq \lambda_2 > 1$ and $\lambda_3 < 1$. If $k_1 = k_2 = k_3 = 1$, the above pseudo-strain-energy function will reduce to the simplest form of the Rivlin series [25, 26]. Further, if $\alpha = 0$, this will correspond to the form of the strain energy function (for a "neo-Hooken" material) derived by Treloar (1943) from *Gaussian* statistics of a network of long chain molecules. When α is larger than 0, this is the famous *Mooney—Rivlin* law for rubber-like materials. For polymer or rubber materials, the range of α is usually between 0 and 0.15 [27].

In this paper, we assume that the *directional microfibrillar stiffening factors*, k_1, k_2 and k_3, are constants which do not vary with the cell wall extension ratios or the cell expansion ratio. Consequently, from Equations 1 and 2 the resulting three principle *Cauchy*

stresses can be derived as

$$\tau_i = k_i G\left(\lambda_i^2 - \frac{\alpha}{\lambda_i^2} - 1 + \alpha\right) + p \qquad (3)$$

where, $G = 2C_1$ is the elastic constant of the cell wall matrix.

The cell walls are permeable to water and some solutes, and the cells are able to hold water under pressure by a high internal concentration of solutes [28]. The turgor pressure (p_c) is the difference between the internal water pressure and the external pressure, which is maintained by osmotic potential of the cells. In hexagonal or cylindrical cells subjected to a positive internal turgor pressure, the cell walls experience about twice as much tensile stress in the circumferential direction as in the axial direction. If the elastic properties of the cell walls are the same in both the axial direction and the circumferential directions, a hexagonal or cylindrical cell would expand radially at a faster rate than it would axially. Thus we have $k_1 > k_2 > k_3 = 1.0$. If no compressive load is applied on the tissue, the initial reduced turgor pressure $\overline{p_{c_i}}$ can be derived from our previous analysis [16], and given by

$$\overline{p_{c_i}} = \frac{p_{c_i}}{k_1\rho_0 G} = \frac{\lambda_{2i}\nu_i^2 - \alpha\lambda_{2i}^3 - \lambda_{2i}^2\nu_i + \alpha\lambda_{2i}^2\nu_i - \beta\left(\lambda_{2i}^4\nu_i - \alpha\nu_i - \lambda_{2i}^2\nu_i + \alpha\lambda_{2i}^2\nu_i\right)}{\lambda_{2i}^2\nu_i^2} \qquad (4)$$

where, $\rho_0 = 2t_0/\sqrt{3}l_0$ is the original cell wall volume fraction (i.e. the cell wall volume over the tissue volume when the turgor pressure is zero, t_0 is the original cell wall thickness and l_0 is the original cell edge length) when the turgor pressure is zero, $\beta = k_2/k_1$ is the ratio of the *axial microfibrillar stiffening factor* to the *circumferential microfibrillar stiffening factor*, α is a material constant of the cell wall [16, 27]. $\nu_i = V_i/V_0 = \lambda_{1i}^2\lambda_{2i}$ is the initial cell volume expansion ratio, λ_{1i} and λ_{2i} are the initial extension ratios respectively in the circumferential direction and the axial direction when no load is applied on the tissue. λ_{1i}, λ_{2i}, ν_i and p_i all can be determined from the previous analysis [16].

When the tissue is compressed (see Fig. 1b), the cell surface area increases, hence the cell wall tension and the turgor pressure will also increase. The increase in turgor pressure will break the osmotic equilibrium and cause cell fluid to flow out through the cell wall at a rate which is proportional to the cell wall permeability D and to the difference between the present turgor pressure p_c and the initial turgor pressure p_{c_i}. Other time-dependent properties of the tissue, such as viscoelasticity or visco-plasticity of the cell walls and the movement of extracellular fluid, are disregarded.

We will use h and s as subscripts to notate respectively the horizontal walls and the slant walls of the cells (see Fig. 1b). The cells are assumed to have a much larger dimension in the axial direction (i.e. direction 2, which is normal to the plane of the paper) than in the circumferential direction (direction 1), hence all the faces in Fig. 1b are assumed to have the same axial extension ratio λ_2 (i.e. $\lambda_{h2} = \lambda_{s2} = \lambda_2$). As discussed in the previous paper [16], when potato or cucumber tissue is treated either by freezing or by heating, the static stiffness of the tissue can be dramatically reduced [1–3] compared with that of the unprocessed one. Since unprocessed potato or cucumber tissue is tens of times statically stiffer than the (freezing or heating) processed tissue, we know that cell wall stretching plays a much more important role than cell wall bending in the compressive deformation of the tissues. Consequently, we assume no interstitial voids present between the cells, the cell walls offer no bending resistance and hence can be treated as hinged at the cell edges. This assumption can greatly simplify the analysis, but does not very much influence the analytical results of the tissues subjected to relatively high loading rate compression. Pitt and Chen also treated the cell walls as hinged at the edges in their paper [19]. The main difference between Pitt and Chen's model [19] and ours is that their model is two dimensional, in which the cell wall material was treated as linear elastic, and *microfibrillar stiffening* was not taken into account.

We will use *Cauchy* stress, τ, in the following analysis unless where specified. When the tissue is subjected to a uniform compressive stress, the characteristic angle Γ will reduce from the original value 60^0, and the principle *Cauchy* stress τ_3 will always equal the cell fluid pressure $-p_i$. From Equation 3 we have

$$\begin{aligned}\tau_1 &= G\left(k_1\left(\lambda_1^2 - \alpha/\lambda_1^2 - 1 + \alpha\right) - \lambda_1^{-2}\lambda_2^{-2}\right.\\ &\qquad \left. + \alpha\lambda_1^2\lambda_2^2 + 1 - \alpha\right) - p_i\\ \tau_2 &= G\left(k_2\left(\lambda_2^2 - \alpha/\lambda_2^2 - 1 + \alpha\right) - \lambda_1^{-2}\lambda_2^{-2}\right.\\ &\qquad \left. + \alpha\lambda_1^2\lambda_2^2 + 1 - \alpha\right) - p_i\end{aligned} \qquad (5)$$

where, $p_i = p_c + p_0 = -\tau_3$ is the fluid pressure inside the cells. Owing to the fact that the original cell wall volume fraction (i.e. the cell wall volume over the tissue volume when $p_c = 0$) ρ_0 is about 0.1 or less [20] and $\lambda_1 \geq \lambda_2 > 1$ and $\lambda_3 < 1$ for the compressed tissue, the cell wall's *Cauchy* stresses τ_1 and τ_2 are usually tens of times larger than the turgor pressure p_c, hence much larger than the fluid pressure p_i. To simplify the analysis, we ignore the term p_i in the above equation and rewrite it as

$$\begin{aligned}\tau_1 &= G\left(k_1\left(\lambda_1^2 - \alpha/\lambda_1^2 - 1 + \alpha\right) - \lambda_1^{-2}\lambda_2^{-2}\right.\\ &\qquad \left. + \alpha\lambda_1^2\lambda_2^2 + 1 - \alpha\right)\\ \tau_2 &= G\left(k_2\left(\lambda_2^2 - \alpha/\lambda_2^2 - 1 + \alpha\right) - \lambda_1^{-2}\lambda_2^{-2}\right.\\ &\qquad \left. + \alpha\lambda_1^2\lambda_2^2 + 1 - \alpha\right)\end{aligned} \qquad (6)$$

The force equilibrium conditions require

$$\tau_{h1}\lambda_{s1} = 2\tau_{s1}\lambda_{h1}\cos\Gamma \qquad (7)$$

$$2\tau_{s2} + \tau_{h2} = 4(\lambda_{h1} + \lambda_{s1}\cos\Gamma)\lambda_{s1}\lambda_2 p_c \sin\Gamma/(\sqrt{3}\rho_0) \qquad (8)$$

and

$$\tau_{h1} = 4p_c\lambda_{h1}\lambda_2\lambda_{s1}\sin\Gamma/(\sqrt{3}\rho_0) \tag{9}$$

If the idealised cell of Fig. 1 is compressed at a constant strain rate $\dot{\epsilon}$, the cell volume expansion ratio ν continuously decreases, hence ν is a dynamic variable and need to be updated with time t. The cell wall extension ratios can be related to the dynamic cell volume expansion ratio ν by

$$4\lambda_2\lambda_{s1}(\lambda_{h1} + \lambda_{s1}\cos\Gamma)\sin\Gamma/(3\sqrt{3}) = \nu \tag{10}$$

Substitution from Equation 6 into Equation 9 gives

$$k_1\left(\lambda_{h1}^2 - \alpha/\lambda_{h1}^2 - 1 + \alpha\right) - \lambda_{h1}^{-2}\lambda_2^{-2} + \alpha\lambda_{h1}^2\lambda_2^2 + 1 - \alpha = 4p_c\lambda_{s1}\lambda_{h1}\lambda_2\sin\Gamma/(\sqrt{3}G\rho_0) \tag{11}$$

From Equations 6, 8 and 10 we have

$$3k_2\left(\lambda_2^2 - \alpha\lambda_2^{-2} - 1 + \alpha\right) - 2\lambda_{s1}^{-2}\lambda_2^{-2} + 2\alpha\lambda_{s1}^2\lambda_2^2 - \lambda_{h1}^{-2}\lambda_2^{-2} + \alpha\lambda_{h1}^2\lambda_2^2 + 3(1-\alpha) = 3p_c\nu/(G\rho_0) \tag{12}$$

From Equations 6, 7 and 11 we can derive

$$k_1\left(\lambda_{s1}^2 - \alpha/\lambda_{s1}^2 - 1 + \alpha\right) - \lambda_{s1}^{-2}\lambda_2^{-2} + \alpha\lambda_{s1}^2\lambda_2^2 + 1 - \alpha = 2p_c\lambda_{s1}^2\lambda_2\tan\Gamma/(\sqrt{3}G\rho_0) \tag{13}$$

In Equations 10–13, the parameters G, α, k_1 and k_2 are material properties and ρ_0 is the initial cell wall volume fraction, and all are assumed to be known for a given species of plant or vegetable tissue. The initial turgor pressure $p_c = p_{c_i}$ for the uncompressed tissue can be measured and the initial cell volume expansion ratio $\nu = \nu_i$ can be derived according to the previous analysis [16]. For a given value of the dynamic cell expansion ratio ν, there are five variables to be determined in the above four Equations 10–13, those are λ_{h1}, λ_{s1}, λ_2, p_c and Γ. Giving a characteristic angle Γ, the other four variables can be solved from Equations 10–13 by an iterative procedure [16].

Assuming that the loading rate is a constant, from Fig. 1b, the compressive strain (engineering strain) of the tissue can be related to the cell wall extension ratio λ_{s1} and the characteristic angle Γ by

$$\epsilon = \dot{\epsilon}t = 1 - \frac{2\lambda_{s1}\sin\Gamma}{\sqrt{3}\lambda_{1i}} \tag{14}$$

where, $\dot{\epsilon}$ is the constant strain loading rate, and t is the loading time. Once a new value of variable λ_{s1} has been solved from Equations 10–13, the characteristic angle Γ can be updated by

$$\Gamma = \sin^{-1}\left((1-\dot{\epsilon}t)\frac{\sqrt{3}\lambda_{1i}}{2\lambda_{s1}}\right) \tag{15}$$

The above process repeated until convergence for a given dynamic cell expansion ratio ν. For a fixed loading rate $\dot{\epsilon}$, once the convergence has been achieved for a given cell volume expansion ratio ν the associated values of λ_2, λ_{s1} and λ_{h1} will all be determined, hence the reduced turgor pressure can be obtained from Equation 12, and given by

$$\begin{aligned}\overline{p_c} &= \frac{p_c}{G\rho_0 k_1} \\ &= \frac{\beta}{\nu}\left(\lambda_2^2 - \alpha\lambda_2^{-2} - 1 + \alpha\right) - \frac{2}{3\lambda_{s1}^2\lambda_2^2\nu k_1} + \frac{2\alpha\lambda_{s1}^2\lambda_2^2}{3\nu k_1} \\ &\quad + \frac{1-\alpha}{\nu k_1} - \frac{1}{3\lambda_{h1}^2\lambda_2^2\nu k_1} + \frac{\alpha\lambda_{h1}^2\lambda_2^2}{3\nu k_1}\end{aligned} \tag{16}$$

The non-dimensional compressive stress (reduced engineering stress) of the tissue is

$$\begin{aligned}\bar{\sigma} &= \frac{\sigma}{G\rho_0 k_1} \\ &= \frac{\overline{p_c}\rho_0 G(\lambda_{h1} + \lambda_{s1}\cos\Gamma)\lambda_2 k_1 - \tau_{s1}t_0\sin\Gamma/(\lambda_{s1}l_0)}{1.5G\rho_0\lambda_{1i}\lambda_{2i}k_1} \\ &= \frac{\overline{p_c}\lambda_2}{1.5\lambda_{1i}\lambda_{2i}}(\lambda_{h1} + \lambda_{s1}\cos\Gamma) - \frac{\sqrt{3}\sin\Gamma}{3\lambda_{1i}\lambda_{2i}\lambda_{s1}k_1} \\ &\quad \times \left[k_1\left(\lambda_{s1}^2 - \alpha\lambda_{s1}^{-2} - 1 + \alpha\right) - \lambda_{s1}^{-2}\lambda_2^{-2} + \alpha\lambda_{s1}^2\lambda_2^2 + 1 - \alpha\right]\end{aligned} \tag{17}$$

and the compressive strain (engineering strain) of the tissue is given in Equation 14. As mentioned before, the parameters λ_{1i} and λ_{2i} in Equations 14 and 17 are the initial cell wall extension ratios in the circumferential direction and the axial direction when no compressive load is applied on the tissue.

In a plant or vegetable tissue, any two neighbouring primary cell walls are glued by a thin layer of middle lamella. When the tissue is subjected to a turgor pressure p_c, there exist tensile forces (or debonding tensions) that arise in the directions perpendicular to each face at the edge and distribute uniformly along the cell edge of unit length. The forces on the slant and horizontal faces are denoted by Q_{s1} and Q_{h1} as shown in Fig. 2b, and given by

$$\begin{aligned}Q_{s1} &= (T_{h1} - T_{s1}\cos\Gamma)/(2\sin\Gamma) \\ Q_{h1} &= (T_{s1} - T_{h1}\cos\Gamma)/(2\sin\Gamma)\end{aligned} \tag{18}$$

where,

$$\begin{aligned}T_{s1} &= T_{s1}t_0\lambda_{s3}\lambda_{s2}/\lambda_2 = \tau_{s1}t_0/(\lambda_2\lambda_{s1}) \\ T_{h1} &= T_{h1}t_0\lambda_{h3}\lambda_{h2}/\lambda_2 = \tau_{h1}t_0/(\lambda_2\lambda_{h1})\end{aligned} \tag{19}$$

Equation 18 shows that Q_{s1} is a tensile force to separate the two neighbouring cells, which increases with the compressive strain ϵ, Q_{h1} is initially equal to Q_{s1}, then decreases with the increasing compressive strain ϵ and becomes smaller than 0. The overall non-dimensional shear stress (engineering stress) on the slant cell faces

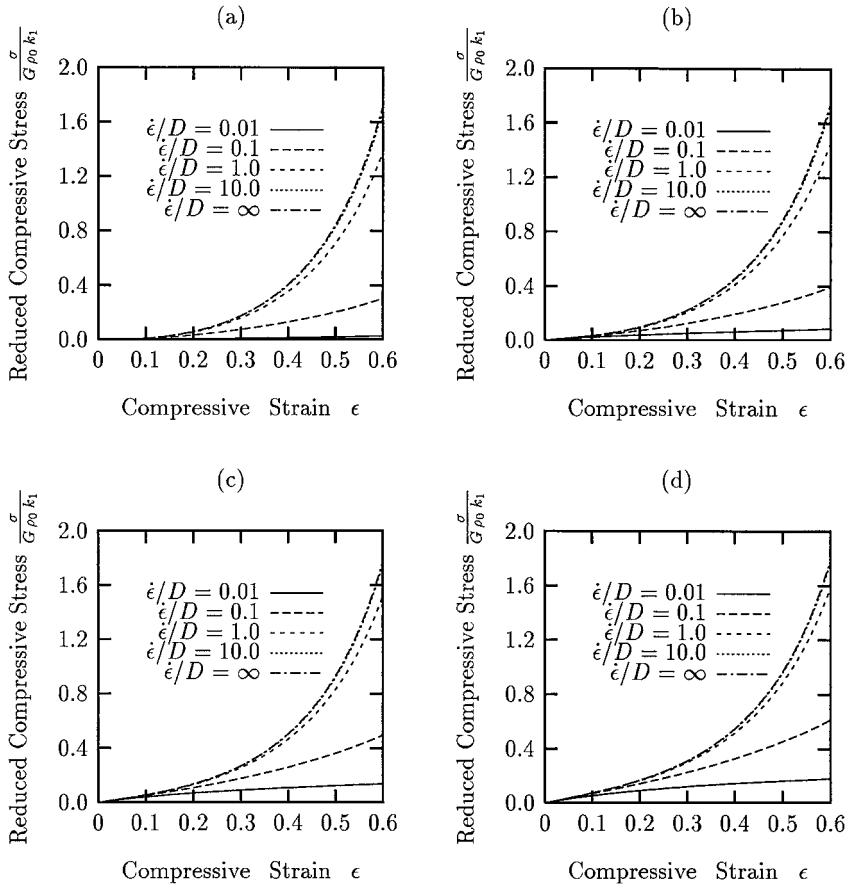

Figure 2 Effects of relative loading rate $\dot{\epsilon}/D$ and the initial turgor pressure on the reduced compressive stress strain relationship of plant or vegetable tissues: (a) $\overline{p_{c_i}} = 0.0$, (b) $\overline{p_{c_i}} = 0.05$, (c) $\overline{p_{c_i}} = 0.1$, (d) $\overline{p_{c_i}} = 0.15$.

(on the adhesive layer between the two neighbouring primary cell walls) is

$$\overline{S_{s1}} = \frac{1}{\lambda_{2i}\lambda_{1i}G\rho_0 k_1}(p_c\lambda_2\lambda_{s1} - 2Q_{s1}\lambda_2/l_0)\tan\Gamma \quad (20)$$

As mentioned before, when a plant or vegetable tissue of Fig. 1 is compressed at a fixed loading rate $\dot{\epsilon}$, the cell expansion ratio ν continuously decreases with the increasing compressive strain ϵ or the time t, and is therefore a dynamic variable. The problem then becomes one of calculating updated values of the cell expansion ratio ν to substitute into Equation 10 as the tissue is compressed at a constant strain rate. Corresponding to a given dynamic cell expansion ratio ν, the weight loss percentage of the cell fluid is

$$\bar{W} = \left(1 - \frac{\nu}{\nu_i}\right) \times 100 \quad (21)$$

where, ν_i is the initial cell expansion ratio when the tissue is not compressed.

As a cylindric sample of plant or vegetable tissue is compressed by two parallel plates, the cell fluid can only express from the cylindric surface. The instantaneous rate of change of the cell expansion ratio ν is approximately proportional to the cell wall permeability coefficient D, the difference between turgor pressure p_c and the initial turgor pressure p_{c_i}, and the ratio of the sample surface area to the sample diameter, and given by

$$\frac{\mathrm{d}\nu}{\mathrm{d}t} = -D\sqrt{\lambda_2(\lambda_{h1} + \lambda_{s1}\cos\Gamma)}\,\lambda_{s1}\sin\Gamma(p_c - p_{c_i}) \quad (22)$$

The numerical technique for the model is to simulate the compression of a lattice of identical 3D hexagonal cells at a constant compressive strain rate $\dot{\epsilon}$, and to calculate the values of $\bar{\sigma}$, $\overline{p_c}$, $\overline{\tau_{h1}}$, $\overline{Q_s}$, $\overline{S_{s1}}$, and $\bar{W}$ at discrete time intervals (i.e. at different compressive strains). At each time interval, a Runge–Kutta method is used to estimate a new value of the cell expansion ratio ν.

It should be noted that, although the microfibrillar stiffening factors k_1 and k_2 have been taken into account in the model, they were treated as constants in the above analysis. In nature, the cell wall microfibrillar stiffening is usually very complex. However, as long as the *microfibrillar stiffening* properties k_1 and k_2 are derived as functions of the cell wall extension ratios λ_1, λ_2 and λ_3, the pseudo-strain-energy function of the cell wall material can be given in the form of Equation 2, then the constitutive relations of the cell wall material can be derived from Equations 1 and 2. Consequently, all the mechanical properties discussed in this paper can be obtained either by an analytic approach or by a numerical method along the lines of this analysis. In addition, Equation 22 presumes that there is no vertical crack in the tissue during the compression, hence, the results are valid only for compressive strains before failure occurs. Owing to the fact that the experimentally

measured results could be greatly different for different plant and vegetable tissues, we did not attempt to fit the model to any special experimental results.

3. Results and discussion

The analysis is focused on the mechanical properties of a plant or vegetable tissue rather than a complete plant or vegetable (which has different structures in different parts). Our main objective is to investigate the effects of varying cell wall permeability D and loading rate (strain rate) $\dot{\epsilon}$ on the mechanical behaviour of plant or vegetable tissues, hence we will fix the cell wall *microfibrillar stiffening factors* at $k_1 = 5$, $k_2 = 2$ and $k_3 = 1$ and the cell wall matrix property at $\alpha = 0.1$ in this paper. It has been assumed that the original cell volume fraction *rho* is 0.1 or less [20], hence cell face stretching is the main deformation mechanism. Owing to the fact that all the results shown in the diagrams have been normalised, they are independent of the original cell volume fraction *rho*.

One may intuitively expect that increasing the cell wall permeability coefficient D will allow cell fluid to express more freely and hence will lower the resistance of the tissue to compression; increasing the loading rate (strain rate) $\dot{\epsilon}$ will give the cell fluid less time to migrate out of the cell, hence help the cell turgor pressure to be built up and thus increase the tissue stiffness. However, as reported by Pitt and Chen [19], we also found that the response of a plant or vegetable tissue to compression depends on the ratio $\dot{\epsilon}/D$ rather than the values of $\dot{\epsilon}$ and D independently—although this result is very difficult to prove mathematically from the model formulation. Pitt and Chen [19] call the ratio $\dot{\epsilon}/D$ the relative strain rate. In addition, we believe that the size of the tissue samples has very modest effect on the results because, firstly as long as the compressive strain rate $\dot{\epsilon}$ is the same, the height of the samples makes no difference on the results (to remain the same compressive strain rate $\dot{\epsilon}$, the compression speed should be larger for the bigger sample than that for a smaller one); secondly the weight loss percentage of a tissue is directly proportional to the surface area and inversely proportional to the diameter, if the height of the sample is a unit and the fluid can not express from the top and the bottom surfaces, the ratio of the cylindric surface of the tissue to the tissue diameter is a constant.

In a plant or vegetable tissue with idealised 3D hexagonal cells, Fig. 2a–d show the reduced stress-strain relationship for four values of the reduced initial turgor pressure $\overline{p_{c_i}}$ and various values of the relative strain rate $\dot{\epsilon}/D$. For each fixed reduced initial turgor pressure $\overline{p_{c_i}}$, increasing the relative strain rate $\dot{\epsilon}/D$ causes the tissue stiffness to increase. When $\dot{\epsilon}/D = 10$ or larger, the reduced stress-strain relationship becomes the same as that of the elastic case in which the cell wall is impermeable to cell fluid (i.e. $D = 0$). The larger the initial turgor pressure, the stiffer will be the plant or vegetable tissue [16]. As observed by Pitt and Chen [19], reducing the relative strain rate $\dot{\epsilon}/D$ causes the reduced stress-strain curve to change from concave-up to concave-down, hence, it may be postulated that there exists a critical relative strain rate at which compressive stress strain relationship will be approximately linear. Consequently, it may be possible to devise a set of compression tests in which cell wall permeability D may be estimated by varying strain rate $\dot{\epsilon}$ until an approximately linear curve is obtained [19]. The slope of this linear curve would then depend on the initial reduced turgor pressure, as shown in Fig. 2a–d.

Fig. 3a–d show the reduced turgor pressure $\overline{p_c}$ versus the tissue compressive strain ϵ for four values of the reduced initial turgor pressure $\overline{p_{c_i}}$ and various values of the relative strain rate $\dot{\epsilon}/D$. For each fixed reduced initial turgor pressure $\overline{p_{c_i}}$, the larger the relative strain rate $\dot{\epsilon}/D$, the higher will be the turgor pressure $\overline{p_c}$. When $\dot{\epsilon}/D = 10$ or larger, the $\overline{p_c} - \epsilon$ relationship becomes almost the same as that of the elastic case in which the cell wall is impermeable to cell fluid (i.e. $D = 0$). In contrast, when $\dot{\epsilon}/D = 0.01$ or smaller, the reduced turgor pressure $\overline{p_c}$ will remain approximately the same level as the initial turgor pressure $\overline{p_{c_i}}$.

Fig. 4a–d illustrate the reduced cell wall stress $\overline{\tau_{h1}}$ versus the tissue compressive strain ϵ for four values of the reduced initial turgor pressure $\overline{p_{c_i}}$ and various values of the relative strain rate $\dot{\epsilon}/D$. Since $\overline{\tau_{h1}}$ is larger than $\overline{\tau_{s1}}$ (see Equation 7), we present results only for $\overline{\tau_{h1}}$, i.e., the maximum reduced principle *Cauchy* stress. Fig. 4a–d show that higher initial reduced turgor pressure $\overline{p_{c_i}}$ results in greater cell wall stresses at a given applied strain. As observed by Pitt and Chen [15, 19] and Zhu and Melrose [16], for a given cell wall breaking stress, the applied strain at cell wall failure will decrease with increasing initial cell turgor pressure because the cell walls are in highly pre-stressed state before any external loads are applied. Thus, increased initial turgidity causes lower tissue strength. As can be seen in Fig. 4a–d, the $\overline{\tau_{h1}} - \epsilon$ curve changes from concave-up to concave-down with decreasing relative strain rate $\dot{\epsilon}/D$. For low relative strain rates $\dot{\epsilon}/D$, the cell wall stress or strain increases gradually, then reaches a maximum, and then actually decreases (or relaxes) as the tissue compressive strain ϵ increases. Thus, there exists a peak point on the $\overline{\tau_{h1}} - \epsilon$ curve if the relative strain rate is small. As $\dot{\epsilon}/D$ decreases, this peak point is achieved at lower strains [19]. If this peak stress is smaller than the cell wall breaking stress, cell wall rupture will never take place.

Fig. 5a–d show the effects of relative strain rate $\dot{\epsilon}/D$ on the relationship between the reduced debonding tension $\overline{Q_s}$ and the tissue compressive strain ϵ. Since $\overline{Q_h}$ initially equals $\overline{Q_s}$ and then decreases with increasing strain ϵ, we present results only for $\overline{Q_s}$. As can be seen in Fig. 5a–d, the higher the initial reduced turgor pressure $\overline{p_{c_i}}$, the larger will be the reduced debonding tension $\overline{Q_s}$. This suggests that in plant high turgor pressure could cause cell debonding. In some cooked food or vegetables, such as potato, the turgor is replaced by swelling of gelatinized starch inside the cells [29], the cells could be separated by the starch swelling pressure. If the starch swelling pressure is not high enough, applying a compressive stress on the cooked potato could help to separate the potato cells. The relative strain rate $\dot{\epsilon}/D$ also strongly affects the $\overline{Q_s} - \epsilon$ relationship: the

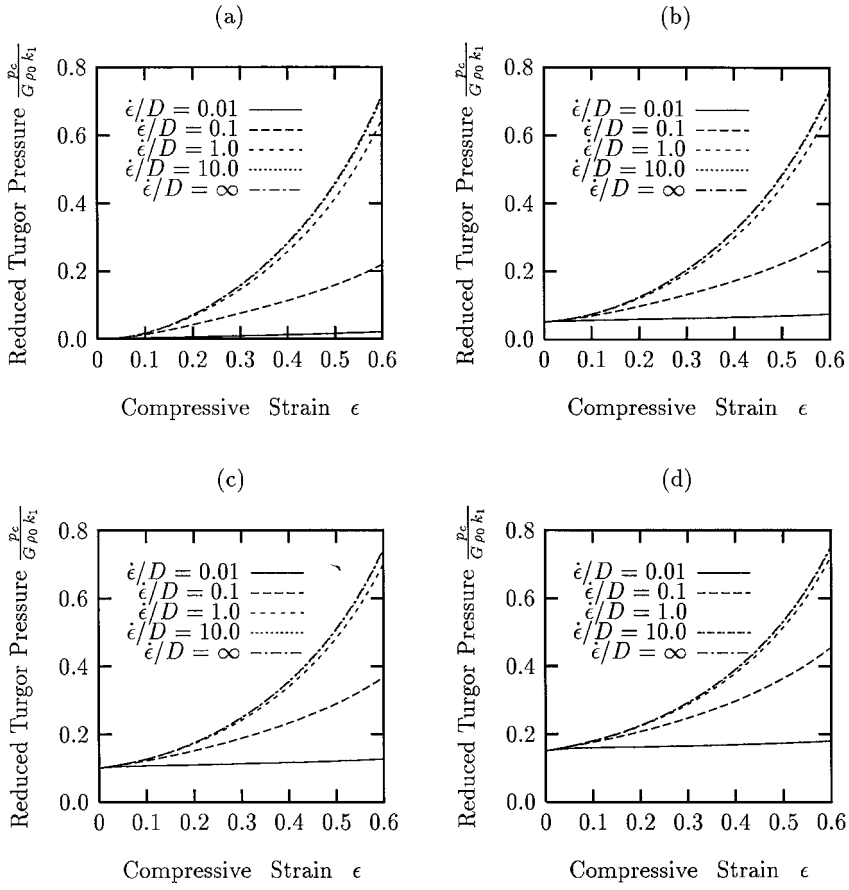

Figure 3 Effects of relative loading rate $\dot{\epsilon}/D$ and the initial turgor pressure on the relationship between the reduced turgor pressure and the compressive strain of plant or vegetable tissues: (a) $\overline{p_{c_i}} = 0.0$, (b) $\overline{p_{c_i}} = 0.05$, (c) $\overline{p_{c_i}} = 0.1$, (d) $\overline{p_{c_i}} = 0.15$.

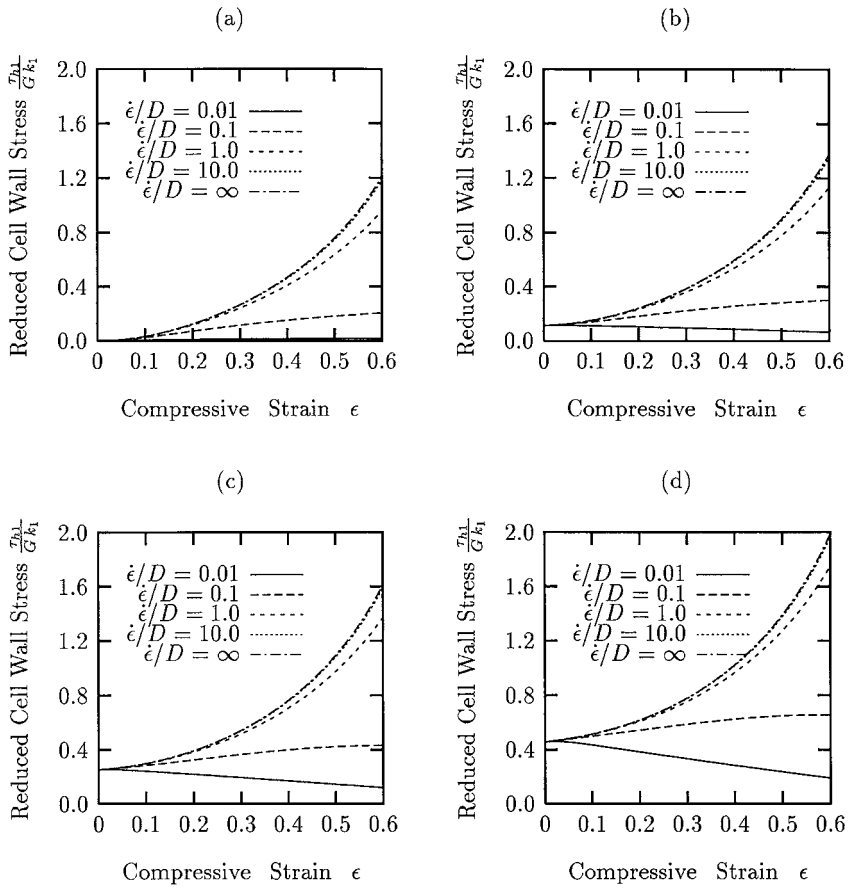

Figure 4 Effects of relative loading rate $\dot{\epsilon}/D$ and the initial turgor pressure on the relationship between the reduced cell wall tensile stress and the compressive strain of plant or vegetable tissues: (a) $\overline{p_{c_i}} = 0.0$, (b) $\overline{p_{c_i}} = 0.05$, (c) $\overline{p_{c_i}} = 0.1$, (d) $\overline{p_{c_i}} = 0.15$.

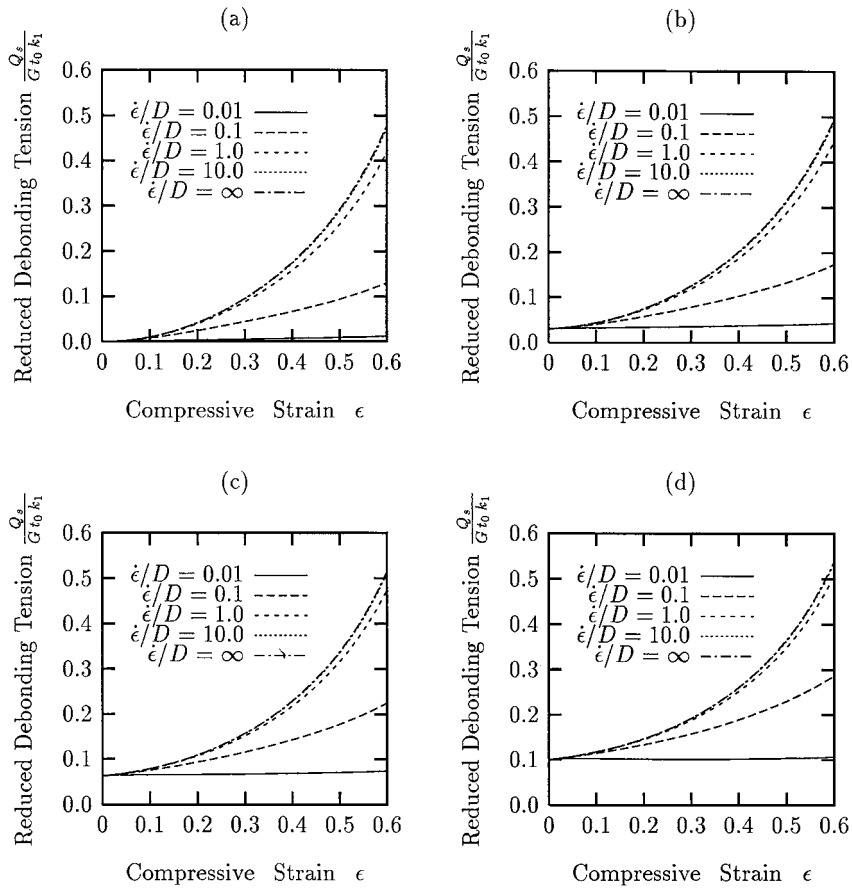

Figure 5 Effects of relative loading rate $\dot{\epsilon}/D$ and the initial turgor pressure on the relationship between the reduced cell face debonding tension and the compressive strain of plant or vegetable tissues: (a) $\overline{p_{c_i}} = 0.0$, (b) $\overline{p_{c_i}} = 0.05$, (c) $\overline{p_{c_i}} = 0.1$, (d) $\overline{p_{c_i}} = 0.15$.

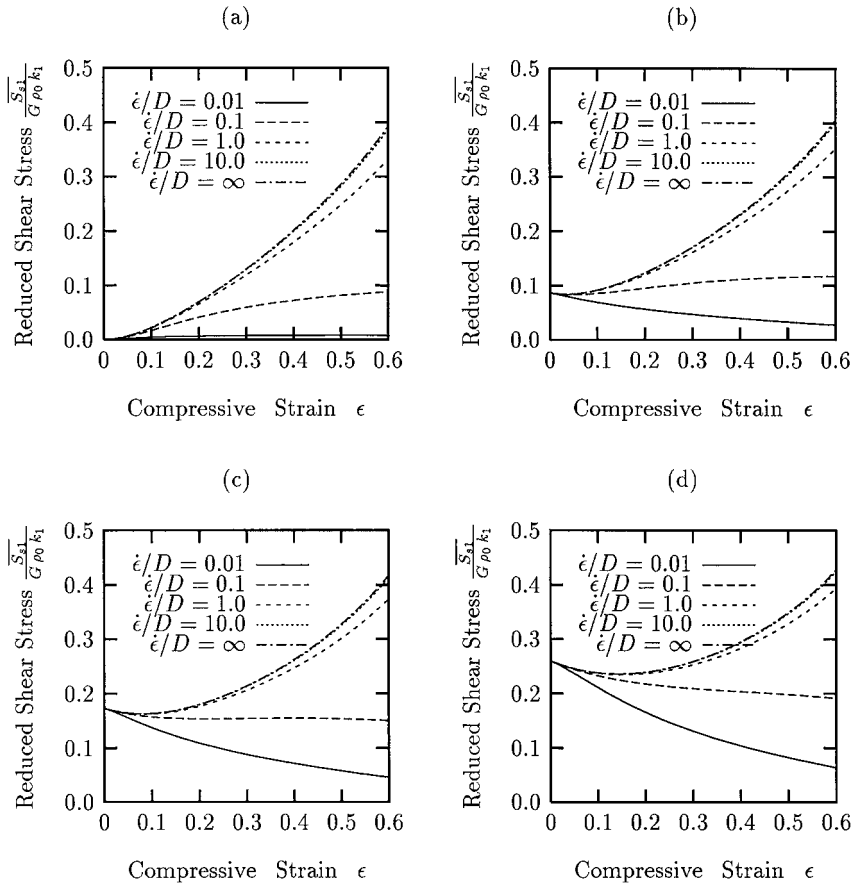

Figure 6 Effects of relative loading rate $\dot{\epsilon}/D$ and the initial turgor pressure on the relationship between the mean reduced shear stress and the compressive strain of plant or vegetable tissues: (a) $\overline{p_{c_i}} = 0.0$, (b) $\overline{p_{c_i}} = 0.05$, (c) $\overline{p_{c_i}} = 0.1$, (d) $\overline{p_{c_i}} = 0.15$.

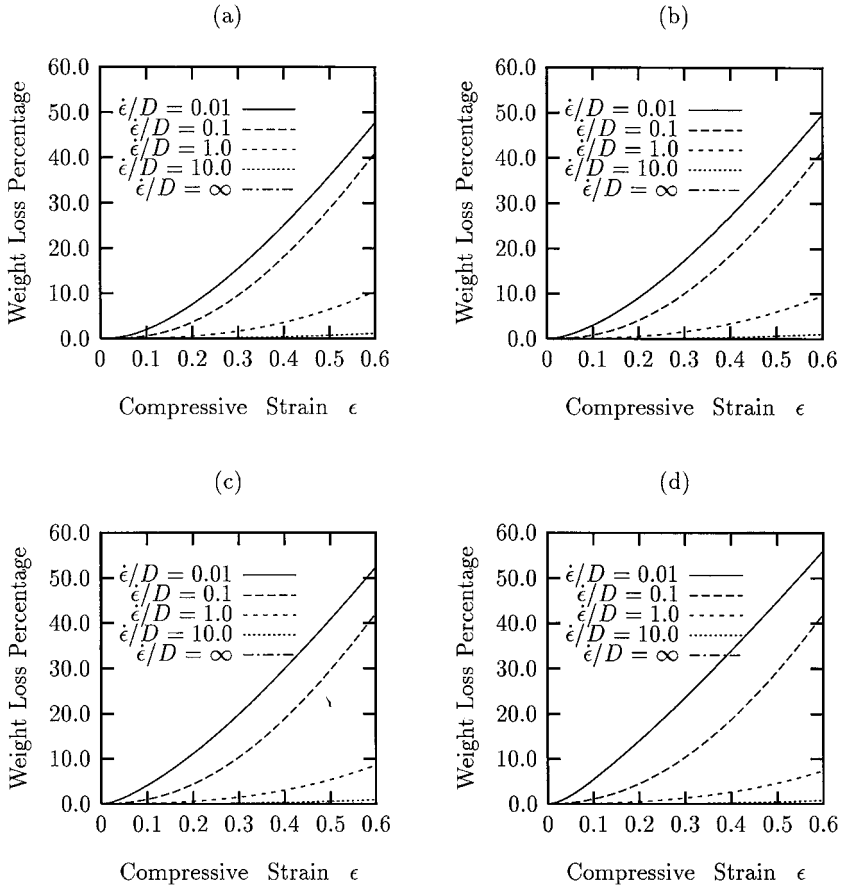

Figure 7 Effects of relative loading rate $\dot{\epsilon}/D$ and the initial turgor pressure on the relationship between the weight loss percentage by fluid expression and the compressive strain of plant or vegetable tissues: (a) $\overline{p_{c_i}} = 0.0$, (b) $\overline{p_{c_i}} = 0.05$, (c) $\overline{p_{c_i}} = 0.1$, (d) $\overline{p_{c_i}} = 0.15$.

larger the relative strain rate, the greater will be the debonding tension. When $\dot{\epsilon}/D$ equals 10.0 or larger, the debonding tension tends to that of the elastic case in which the cell wall is impermeable to cell fluid (i.e. $D = 0$). On the other hand, when $\dot{\epsilon}/D$ equals 0.01 or smaller, $\dot{\epsilon}/D$ will no longer influence the $\overline{Q_s} - \epsilon$ relationship. In this case, compressing the tissue will never result in cell debonding.

Equation 20 is the overall non-dimensional shear stress ($\overline{S_{s1}}$) on the adhesive layer between the two slant neighbouring primary cell walls. For a turgid or compressed tissue, as long as cell debonding does not happen, cell debonding tension $\overline{Q_s}$ always exists. In this case, the overall non-dimensional shear stress remains zero or very small. However, once cell debonding has initiated, cell debonding tension $\overline{Q_s}$ drops very sharply, this will cause a sudden increase of the overall shear stress $\overline{S_{s1}}$. This implies that cell debonding could cause shear failure. In other words, shear failure is a result of cell debonding. Equations 18 and 20 and Fig. 6a–d can well explain the phenomenon when you compress a ripen banana tissue. The deformation mechanism of the tissue is that the cells are debonded initially by debonding tension (Equation 18), then consequently deformed by shear stress (Equation 20). Experimental evidence of shear failure can also be found when an apple tissue is subjected to a large compressive stress [6]. Assuming that the cell debonding tension $\overline{Q_s}$ is zero, Fig. 6a–d present the reduced shear stress $\overline{S_{s1}}$ versus the tissue compressive strain ϵ for four values of the reduced initial turgor pressure $\overline{p_{c_i}}$ and various values of the relative strain rate $\dot{\epsilon}/D$. As can be seen in Fig. 6a–d, the higher the initial reduced turgor pressure $\overline{p_{c_i}}$, the greater will be the reduced shear stress $\overline{S_{s1}}$; the higher the relative strain rate $\dot{\epsilon}/D$, the larger will be the reduced shear stress $\overline{S_{s1}}$. For plant or vegetable tissues with an initial turgor pressure (i.e. $\overline{p_{c_i}} > 0$), if the relative strain rate is very small, the overall shear stress on the slant neighbouring primary cell walls will decrease with increasing compressive strain, this means shear failure will never happen.

As the cell walls are permeable, the cell fluid will migrate out from the tissue as it is compressed. Fig. 7a–d show the amount of fluid expressed from the tissue versus the tissue compressive strain for four values of the reduced initial turgor pressure $\overline{p_{c_i}}$ and various values of the relative strain rate $\dot{\epsilon}/D$. The lower the relative strain rate, the greater amount of the fluid will express from the tissue. While, the initial turgor pressure $\overline{p_{c_i}}$ has a very modest influence on the fluid expression.

4. Summary

A mechanical model was developed for plant or vegetable tissues, relating the micro mechanical features of the individual cells to the macroscopic properties of the whole tissue. The cell walls were treated as a permeable and orthotropic polymeric composite material. Since the stiffening of the microfibrils can be incorporated into the pseudo-strain energy function of the cell wall material, the model can potentially deal with more realistic plant and vegetable tissues. Although the

actual compression situation of a plant or vegetable tissue was greatly simplified in the analysis, the results can well explain some experimental phenomena, and hence should give qualitative insight into the mechanical response of the actual tissue.

The model predicts that the mechanical response of a plant or vegetable tissue depends on the relative strain rate $\dot{\epsilon}/D$ rather than the values of $\dot{\epsilon}$ or D independently. With decreasing relative strain rate $\dot{\epsilon}/D$, the compressive stress-strain curve of a tissue changes from concave-up to concave-down, hence, it may be postulated that there exists a critical relative strain rate at which the compressive stress strain relationship of the tissue will be approximately linear. Increasing turgor pressure or enlarging relative strain rate $\dot{\epsilon}/D$ gives greater apparent tissue stiffness. The turgor pressure and the cell wall permeability may be estimated from the effective mechanical properties of the tissue [19]. The model also predicts that the cell turgor pressure always increases with the tissue compressive strain if the the relative strain rate does not drop. As long as no failure (such as cell wall rupture, cell debonding, or shear failure) occurs in the tissue, the tissue compressive stress always increases with the compressive strain. If the cell wall stress or strain does not relax, increasing the initial turgor pressure decreases the stress or strain at cell wall rupture. Increasing relative loading rate decreases the cell fluid expression and increases the the possibility of cell debonding and shear failure. Generally shear failure coexists with cell debonding.

References

1. A. A. KHAN and J. F. V. VINCENT, *J. Text. Studies* **27** (1996) 143.
2. M. WARNER, B. L. THIEL and A. M. DONALD, *P. Natl. Acad. Sci. USA* **97** (2000) 1370.
3. B. L. THIEL and A. M. DONALD, *J. Text. Studies* **31** (2000) 437.
4. K. C. DIEHL, D. D. HAMANN and J. K. WHITFIELD, *ibid.* **10** (1979) 371.
5. K. C. DIEHL and D. D. HAMANN, *ibid.* **10** (1979) 401.
6. A. A. KHAN and J. F. V. VINCENT, *ibid.* **24** (1993) 423.
7. M. G. SCALON and A. E. LONG, *Food Research International* **28** (1995) 397.
8. S. LURIE and A. NUSSINOVITCH, *Int. J. Food Sci. and Tech.* **31** (1996) 1.
9. L. C. GREVE, R. N. McARDLE, J. R. GOHLK and J. M. LABAVITCH, *J. Agric. Food Chem.* **42** (1994) 2900.
10. K. R. LANGLEY and R. J. MARSHALL, *J. Text. Studies* **24** (1993) 11.
11. O. PLESH, B. BISHOP and W. D. McCALL, *J. Biomechanics* **26** (1993) 243.
12. E. TORNBERG, S. FJELKNER-MODIG, H. RUDERUS, P.-O. GLANTZ, K. RANDOW and D. STAFFORD, *J. Food Sci.* **50** (1985) 1059.
13. S. B. NILSSON, C. H. HERTZ and S. FALK, *Physiologia Plantarum* **11** (1958) 818.
14. H. MURASE, G. E. MERVA and L. J. SEGERLIND, *Trans. of the ASAE* **23** (1980) 794.
15. R. E. PITT, *Trans. of the ASAE* **25** (1982) 1776.
16. H. X. ZHU and J. R. MELROSE, submitted.
17. J. DE BAERDEMAEKER, L. J. SEGERLIND, H. MURASE and G. E. MERVA, ASAE paper No. 78-3057, ASAE, St. Joseph, MI 49085, 1978.
18. I. M. DAL FABBRO, H. MURASE and L. J. SEGERLIND, ASAE paper No. 80-3048, ASAE, St. Joseph, MI 49085, 1980.
19. R. E. PITT and H. L. CHEN, *Trans. of the ASAE* **26** (1983) 1275.
20. K. ESAU, "Plant Anatomy" (John Wiley and Sons, New York, 1965).
21. H. WU, R. D. SPENCE, J. H. SHARPE and J. D. GOESCHL, *Plant, Cell Environ.* **8** (1985) 563.
22. H. WU, R. D. SPENCE and J. H. SHARPE, *J. Theor. Biol.* **133** (1988) 239.
23. R. D. PRESTON, "The Physical Biology of Plant Cell Walls" (Chapman Hall, London, 1974).
24. A. E. GREEN and J. E. ADKINS, "Large Elastic Deformations" (Clarendon Press, Oxford, 1970).
25. R. S. RIVLIN, *Phil. Trans. R. Lond.* A **241** (1948) 379.
26. M. MOONEY, *J. Appl. Phys.* **11** (1940) 582.
27. L. R. G. TRELOAR, "The Physics of Rubber Elasticity" (Oxford Press, Oxford, 1975).
28. P. S. NOBEL, "Introduction to Biophysical Plant Physiology" (W. H. Freeman, San Francisco, CA, 1974).
29. M. C. JARVIS, *Plant. Cell and Environment* **21** (1998) 1307.

Received 1 January
and accepted 17 October 2002